Oil and Organic Liquids Incorporation into Fresh Geopolymer Pastes Using Suitable Quaternary Ammonium Surfactants.

Christel Pierlot, Yann Boland, Hanyu Hu, Charles Reeb, Jordan Bassetti, David Lambertin

Journal of Oleo Science

doi : 10.5650/jos.ess23183
J. Oleo Sci. **73**, *(4) 625-636 (2024)*

Oil and Organic Liquids Incorporation into Fresh Geopolymer Pastes Using Suitable Quaternary Ammonium Surfactants

Christel Pierlot[1]*, Yann Boland[1], Hanyu Hu[1], Charles Reeb[1,2], Jordan Bassetti[1], and David Lambertin[2]

[1] *Centrale Lille, Université de Lille, CNRS, Université Artois, UMR 8181-UCCS-Unité de Catalyse et Chimie du Solide, Lille, FRANCE*
[2] *CEA, DES, ISEC, DE2D, SEAD, LCBC, Univ Montpellier, Marcoule, FRANCE*

Abstract: The direct incorporation of low viscosity organic liquids (OL) such as dodecane and tributylphosphate (TBP) into fresh geopolymers (GP) is difficult and generally leads to variable amounts of un-incorporated OL remaining outside the hardened geopolymer. Experimentally, it is observed that a regular torque increase during OL incorporation corresponds to a suitable dispersion of the OL in the form of fine micrometric droplets. This can be obtained for TBP and dodecane by adding a small quantity of quaternary ammoniums salts (QAs) such as cetyltrimethylammonium bromide (CTAB). Shorter alkyl chains QAs, such as hexamethyltrimethylammonium (HMTA) can also be used but with a reduced efficiency. The positive impact of CTAB is then confirmed by the Washburn capillary rise method, showing that the interactions between TBP and CTAB-modified metakaolin are weaker compared to untreated powder. Finally, it is observed that the incorporation of TBP into geopolymer slurries is much easier than the incorporation of dodecane. The low interfacial tension measured between TBP and the activating solution (around 8 $mN \cdot m^{-1}$), contrasting with dodecane (29 $mN \cdot m^{-1}$), explains that the dispersion of TBP droplets in fresh metakaolin suspensions is more efficient.

Key words: geopolymer, tributylphosphate, dodecane, interfacial tension, washburn

1 Introduction

Geopolymers[1-3] are polymers above all polymeric materials like their organic analogues, and the prefix *geo* is used to indicate that their structure is mineral. Geopolymers, composed of an amorphous three-dimensional inorganic network and synthesized by the activation of a solid alumino-silicate precursor with an alkaline medium, called activating solution, have attracted increasing attention because of their environmental benefits and favorable characteristics. In fact, the production of Portland cement contributes to about 8% of anthropogenic CO_2 emissions[4] and is responsible for about 0.8 tons of CO_2 equivalent per ton produced. Thus, there is an urgent need for alternatives to Portland cement, to meet the growing demand for infrastructure construction while respecting a reduction in carbon dioxide emissions.

Incorporation of industrial waste into cementitious materials (by the method of stabilization and solidification, also called S/S) is well documented, as it provides assurance of chemical stabilization of many compounds and produces a mechanically stable form of waste. Unfortunately, the stabilization of organic liquids (OL) in Ordinary Portland Cement (OPC) greatly retards and disrupts cement setting, and organic liquids generally form weak chemical bonds in cement unlike some inorganics[5, 6]. Due to these disadvantages, geopolymers could be a solution to replace OPC for the incorporation of organic liquids and also for the treatment of OL waste.

Since the resulting paste hardens to form a solid material (hardened GP), mixing organic liquids (OL) with such aqueous suspensions[1, 2, 7, 8] has been recently described for the synthesis of porosity-controlled media, thermal insulating foams or filtration supports[9-13] and for the treatment of radioactive wastes[14, 15].

In order to understand the immobilization of radioactive organic liquid wastes, alkanes[14, 16] and paraffin oils[17] are used as model oils. The one-step incorporation process, which seems industrially more reasonable than the two-

*Correspondence to: Christel Pierlot, Centrale Lille, Université de Lille, CNRS, Université Artois, UMR 8181-UCCS-Unité de Catalyse et Chimie du Solide, Lille, FRANCE
E-mail: christel.pierlot@univ-lille1.fr
Accepted January 24, 2024 (received for review September 21, 2023)
Journal of Oleo Science ISSN 1345-8957 print / ISSN 1347-3352 online
https://www.jstage.jst.go.jp/browse/jos/ https://mc.manuscriptcentral.com/jjocs
This is the article by the winner of the WCOS 2022 Selected Lecture Award, The Japan Oil Chemists' Society (JOCS).

step process, requires the direct incorporation of the organic liquid into the fresh geopolymer suspension. Organic liquids typically exhibit limited incorporation without the introduction of specific additives. Among these additives, quaternary ammonium surfactants efficiently facilitates the emulsification of OL into GP suspensions. In particular, cetyltrimethylammonium bromide (CTAB) appears to be a promising candidate. It was also observed that when using CTAB, the viscosity of fresh hexadecane/geopolymer composite pastes containing 20% by volume of hexadecane is between 100 and 1000 times higher than the viscosity of the pure geopolymer slurry[18].

The measurement of the viscosity of the reaction medium is generally carried out in offline mode using a rheometer, which very often is not near the reactor. Furthermore, this method is not industrially suitable because it requires constant motions, which are time consuming. On the contrary, the direct torque measurement allows to have an immediate estimation of the viscosity throughout the process and to obtain valuable information when changing formulation parameters.

Thus online torque measurement has already been used to follow emulsification processes of viscous organic polymers such as polyethylene[19], epoxy resin[20], polyurethane[21], polyester[22, 23], rosin resins[24], bisphenol A-polyester[25], silicon resin[26] or bitumen[27].

This article is the continuation of our previous work[30] with a view to completing the interest of online torque monitoring carried out in the reactor before and during the incorporation of organic liquids, and in particular to see the effect of an excess of additive (such as surfactant) in the reaction medium. The objective is to determine to what extent torque tracking provides relevant information on both the oil incorporation process and its distribution in the GP. Another notable modification compared to reference[30] is the study of low viscosity organic fluid, tributylphosphate (TBP) and dodecane. Their low viscosity, implies that their incorporation into fresh GP requires the use of additives. Moreover, the TBP/Dodecane mixture is used as solvent extraction in several industrial processes, such as hydro-metallurgy and industrial nuclear fuel reprocessing (PUREX process).

Different quaternary ammoniums will be evaluated regarding their performance on the incorporation of TBP/Dodecane into geopolymers. The well-known cetyltrimethylammonium (CTAB) will be taken as a reference to determine the effectiveness of other quaternary ammoniums.

2 Experimental Procedures

2.1 Materials

Geopolymers were synthesized using an aluminosilicate source (metakaolin, ARGICAL-M 1000, Imerys), a sodium silicate solution (Woellner, Betol® 39 T: 27.8 wt% SiO_2, 8.3 wt% Na_2O and 63.9 wt% H_2O) and sodium hydroxide (Sigma Aldrich, 99%). Geopolymers have the following molar composition 3.8 SiO_2 : 1 Al_2O_3 : 1 Na_2O : 13 H_2O.

Hexyl-, octyl-, decyl-, dodecyl-, tetradecyl-, hexa-trimethylammonium bromide and Sudan IV as dye were purchased from Sigma-Aldrich. Mineral oils Nevastane EP100 and Finavestan A360B were obtained from Total, Shellspirax S2 A 80W-90 is a commercially available oil. Dodecane, and Tributyl phosphate were obtained from VWR with an announced purity of 99%.

2.2 Geopolymer/oil preparation

The experimental setup used to prepare the fresh suspension of geopolymer and then to incorporate the organic liquid is described in Fig. 1. First, 12.92 g of sodium hydroxide, 82.16 g of Betol® 39 T silicate solution and 11.04 g of deionized water are introduced into a 500 mL reactor to form the activating solution. The mixture was first stirred at 400 rpm with the Heidolph RZR 2051 control to ensure the complete dissolution of sodium hydroxide, and then cooled down during 1 hour to reach room temperature. 72.12 g powder of ARGICAL-M 1000 are dispersed in the aqueous

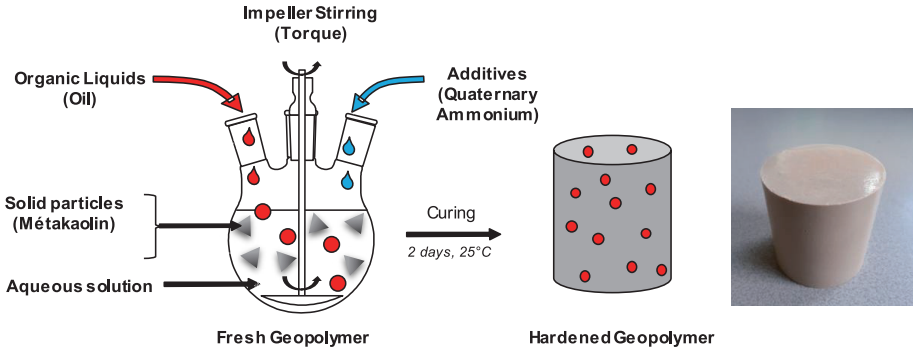

Fig. 1 Experimental setup used to prepare the fresh suspension of geopolymer and then to incorporate the organic liquid. Schematic picture and real aspect of hardened geopolymer with organic liquid droplets inside is represented on the right.

solution during 2 min and the mixture is stirred during 15 min at 800 rpm until both torque stability and visual homogeneity of the dispersion are obtained. At this stage, the fresh geopolymer paste is formulated. The last step consists of introducing the Sudan IV colored organic liquid into the suspension with a Syringe pump Legato (kdScientific) at a flow rate of 4.0 mL.min^{-1}. The fresh suspension is transferred into open cylindrical polystyrene container which is then closed with the lid and aged at room temperature for 2 days before solid-state characterization. While incorporating the organic liquid into the freshly prepared geopolymer, the torque is measured in function of time using a Heidolph RZR 2051 control and recorded via a specific software (Watch/Control 200) pro-vided by Heidolph.

2.3 Rheological experiments

Kinexus rheometer (Malvern) was used with the cone-plate (6 cm, 4°) geometry, 3 mL of the organic liquid or geopolymer suspension is placed inside the gap.

2.4 Torque measurements

Heidolph RZR 2051 control was used to measure the torque in function of time at a selected stirring rate (100 to 800 rpm). Data were recorded via a specific software (Watch/Control 200) provided by Heidolph.

2.5 Optical microscopic analysis

A Keyence VHX-5000 microscope is used in reflection-mode for hardened geopolymer observations. Fresh geopolymers with dispersion in water (1/10) were observed using Axiostar microscope Zeiss in transmission-mode.

2.6 Washburn tests

Krüss Force Tensiometer - K100 was used to perform the Washburn tests in the sorption mode. 1.0 g of powder (natural or hydrophobically modified metakaolin) is introduced in an appropriate sample holder, which is packed using 2 kg weight for 30 seconds. Mass^2 (w^2) versus time (t) data are monitored as soon as the liquid penetrates into the solid.

Hydrophobically metakaolin powders (MK-CTAB) were obtained by dispersing 5.0 g of natural metakaolin in 50 mL aqueous solution of 10^{-2} M CTAB. After stirring during 2 hours, the powders were then filtered on paper and dried in an oven at 60℃ overnight.

2.7 Superficial and interfacial tension

Krüss Tensiometer DSA 10 was used in the pendant droplet software. The denser phase is introduced into the syringe, and the less dense phase (organic liquid) into a small quartz tank (2 × 2 × 2 cm).

3 Results and Discussion

3.1 Experimental setup

Figure 1 represents the experimental setup for forming the geopolymer suspension (with the proportions indicated in 2.2) by adding metakaolin to the activation solution. When the torque value is stabilized, OL is added at a constant rate of 4.0 mL per minute. The addition of OL is stopped as soon as its incorporation into the geopolymer becomes difficult. The mixture is then removed from the reactor and placed within a plastic container to obtain the hardened geopolymer after a few days (photo of the fresh geopolymer on the turbine and hardened in the container, are presented in Fig. 2).

The torque is recorded during the incorporation of the

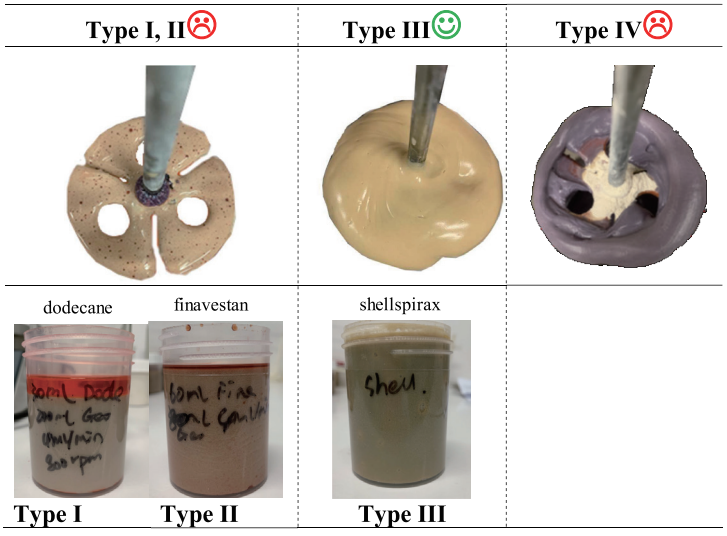

Fig. 2 Visual appearance of the three types (Type I, II and III) of mixture of organic liquid and suspension of metakaolin in the fresh geopolymer (top on the turbine) in the hardened geopolymer (bottom in the plastic container).

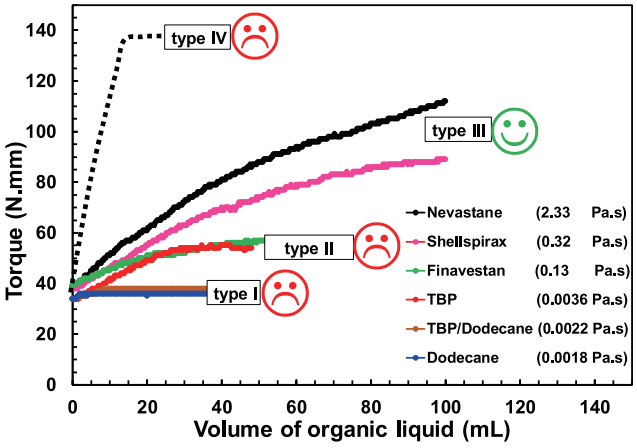

Fig. 3 Torque (N) variation versus organic liquid volume (mL) added at a flow rate of 4.0 mL.min^{-1} at a stirring speed of 800 rpm in 80 mL of fresh geopolymer: Different mineral oil (Nevastane, 2.33 Pa·s; Shellspirax, 0.32 Pa·s), industrial oil (Finavestan, 0.13 Pa·s), two pure organic liquids (Tributylphosphate (TBP), 3.6 mPa·s ; Dodecane, 1.8 mPa·s), a mixture TBP/Dodecane (30/70 w%, 2.2 mPa·s) have been used.

OL (Fig. 3). It can be noticed that the initial state (v = 0.0 mL) which corresponds to the same composition of fresh geopolymer, presents small variations in torque (35-40 N·mm) which can be attributed to a slight change in the position of the impeller in the reactor. But this difference of 5.0 N·mm is negligible compared to the variation in torque obtained during the incorporation of OL. Moreover, even if there are small variations in torque due to the positioning of the turbine in the reactor, it should be noted that the initial value of the torque (before the addition of organic liquid) is stable over time. And, it is the same at the end of the addition of the organic liquid. Finally, by precisely controlling both the stirring speed and the organic liquid addition rate, the torque measurements can be considered reproducible, within the range of experimental error.

Depending of the type of organic liquid (OL) that is incorporated, four torque evolution profiles (Fig. 3) can be distinguished (Type I, II, III or IV) whose corresponding GEOIL (geopolymer and incorporated organic liquid) aspect are presented in Fig. 2 before and after hardening. In the case of dodecane or TBP/dodecane, the torque remains constant. The torque recording was proceeded until introduction of 40 mL of OL, but in fact, the oil incorporation into the GP was not taking place. After stopping the agitation, the organic liquid directly coalesced at the surface of the GP. The small amount of OL that is being incorporated is in the form of big droplets of a few millimeters diameter, as can be seen on the picture of the paste (Fig. 2, first column). In the end, the paste corresponds practically to the fresh geopolymer in terms of viscosity and is defined as type I GEOIL. After breaking the hardened GEOIL into small pieces using a hammer, microscopic examination (Fig. 4) of a small fragment allows to see the oil dispersion inside the solid matrix. For dodecane, only a few very small droplets of a few microns are visible (red dotted circle in Fig. 4A). This indicates that practically no dodecane are incorporated (all the coalesced dodecane was found on the surface of the GEOIL).

In the case of TBP and Finavestan, the torque increases regularly up to 54 N·mm and then stabilizes. This late torque stabilization results from the limit of incorporation and the fresh paste is still too fluid to avoid small coalescence of OL droplets on the surface (Fig. 2 for Finavestan). This is confirmed by a very heterogeneous distribution of TBP drops (red dotted circles) trapped in the hardened geopolymer (Fig. 4B), and in particular the presence of excessively large droplets (150 microns). GEOIL type II will characterize such systems.

In the case of Nevastane and Shellspirax mineral oils, the torque increases constantly even after adding 100 mL of oil and the dispersion seems macroscopically very homogeneous as shown by the appearance of the GEOIL on the impeller. GEOIL type III will characterize such behavior. The microscopic state (picture not presented) shows the dispersion of numerous oil droplets ranging from 1.0 to 50 microns.

A last behavior can be observed when the viscosity of the medium (and therefore the torque) increases too quickly (type IV, Figs. 3 and 4). In this scenario, the reaction medium is not correctly homogenized, since the

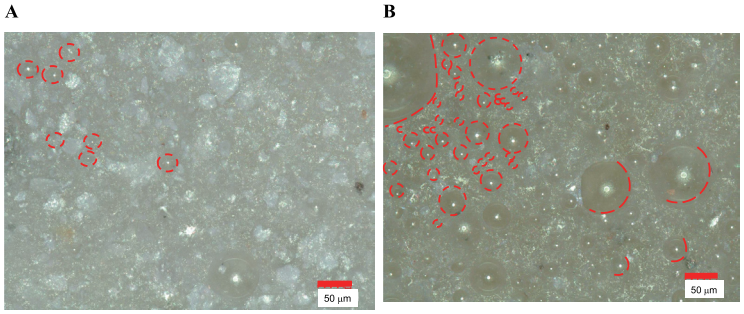

Fig. 4 Optical microscopy in reflection mode of hardened GEOIL with 23% of incorporated dodecane (A) and TBP (B).

turbine is in motion but fails to propel the geopolymer. Consequently, the geopolymer is unable to achieve the required flow for packaging into the plastic container.

With regard to the Fig. 3, it seems that if the OL viscosity is greater than 0.13 Pa·s (Nevastane or Shellspirax), the incorporation into the geopolymer is done relatively well. If the viscosity is about 0.13 Pa·s, such as Finavestan oil, the incorporation of OL will be possible but with relatively large droplet sizes and also in limited quantity, if the formulation of the reaction medium is not revised. For OLs with very low viscosities (less than 0.004 Pa·s) such as TBP, dodecane and their mixtures, the incorporation is not possible without modifying the formulation of the reaction medium.

Several methods exist for the incorporation of OL into geoplymers[29]. The direct route (OL is directly poured into the fresh GP slurry) is easy to implement, and large amounts of OL can be incorporated. The viscosity of geopolymer slurries generally helps to prevent coalescence of OL droplets formed by mechanical stirring until hardening of the paste. However, at high incorporation rates and for low viscosity OL[30], coalescence of OL droplets becomes more favorable, and this leads to phase separation. In such cases, the addition of surfactants can be necessary to maintain emulsion stability.

Cationic[31] and non-ionic[32] surfactants have proven their effectiveness for the incorporation of OL in geopolymers. Surfactants reduce the size of dispersed droplets by decreasing the interfacial tension, which slows down the droplet movements and stabilizes the emulsion. Moreover, surfactants are also organic molecules with versatile chemical structures, so they can adsorb at the surface of solid metakaolin and induce a stabilization of OL droplets. In the latter case, they can structure the oil/geopolymers fresh mixes, with greater viscosity than without surfactant[33]. To be more precise, cationic (CTAB), anionic (Sodium dodecyl sulfate (SDS)), and non-ionic surfactants (Span 80, Tween 80, Brij O10 and Alkylpolyglucoside (Glucopon)) have already been tested as an agent for incorporating organic liquids in geopolymers in our previous work[33]. In mechanism of action 1, the surfactant simply reduces the oil droplet size by decreasing the interfacial tension. This is the classical way for emulsions formulation. The metakaolin particles don't have a direct influence on the stability of the oil droplets. In this mechanism 1, the surfactants only have to be soluble enough in the activating solution to reduce the interfacial tension, by positioning themselves at the interface between both liquids. For mechanism 2, surfactants need to be poorly soluble in the aqueous phase and able to absorb at the surface of the solid particles via their polar heads. While the lipophilic parts of the surfactants remain in contact with the droplets of organic liquid, the connection between the solid particles and the oil droplets create a kind of network which causes an increase in the viscosity of the medium. This is often the case with quaternary ammoniums such as CTAB, and Span 80. Since anionic surfactants like SDS are unable of adsorbing at the surface of kaolin in alkaline conditions because electrical repulsion, and since glucopon are not salts sensible are totally soluble in aqueous media, these two last surfactants act as mechanism 1.

The constraint of the low viscosity of TBP and dodecane for solidification/stabilization (S/S) into geopolymers has already been observed by some authors[34]. These latter found that incorporation can be achieved by assembling a high viscosity organic (oil or grease) with the low viscosity OL, before mixing with the fresh GP.

3.2 Incorporation of TBP/Dodecane in GP using quaternary ammonium salts

To see to what extent the incorporation of TBP/dodecane could be improved using surfactants, we focused on a particular class of surfactants which are quaternary ammoniums salts (QAs). QAs have been already used to improve the compressive strength[31] or to obtain nanoporous solids with high surface area[35–38], to improve the compressive strength of geopolymers[31] or to increase the hydrophobicity of mineral metakaolin particles[39–42]. The interaction between metakaolin and QAs, responsible for an increase in viscosity of fresh geopolymers has already been observed when using cetyltrimethylammonium bromide (CTAB)[43, 44].

Beneficial effect of CTAB on the incorporation of a moderately viscous oil[30] has been already shown, thus this surfactant will be used as reference to examine the incorporation of a very fluid oil mixture TBP/dodecane.

Moreover, to see the influence of the hydrophobic part of the QA alkyl chain, we also compared the effect of another surfactant with an octyl chain. Both CTAB (C_{16}-TAB) and C_8-TAB will be introduced in the activating solution at different concentrations (0, 1, 3, 5 and 10.10^{-3} M), and the torque evolution during OL introduction is shown in Fig. 5. The black curve in Figs. 5A and 5B (that is also presented in Fig. 3), corresponds to the same experiment without QAs (Type I GEOIL).

Using the calibration curve, correspondence between torque and viscosity was reported in Fig. 5A. Without QAs the viscosity of the GP increases slightly from 1.7 to 2.4 Pa·s (from 35 to 40 N·mm in torque).

In the absence of TBP/dodecane (V = 0 mL) in Figs. 5A and 5B, the effects of CTAB and C_8-TAB are similar since an almost regular increase in torque is observed for the initial slurry from 35 to 55 N·mm with an increase of concentration from 1 to 10.10^{-3} M.

For lower CTAB concentrations of 1.10^{-3} and 3.10^{-3} M, the torque increases sharply up to 5 mL of organic liquid added, then increases again but less rapidly up to 20 mL. The quality of the dispersion is high and corresponds to a type III GEOIL. As observed previously, when the addition

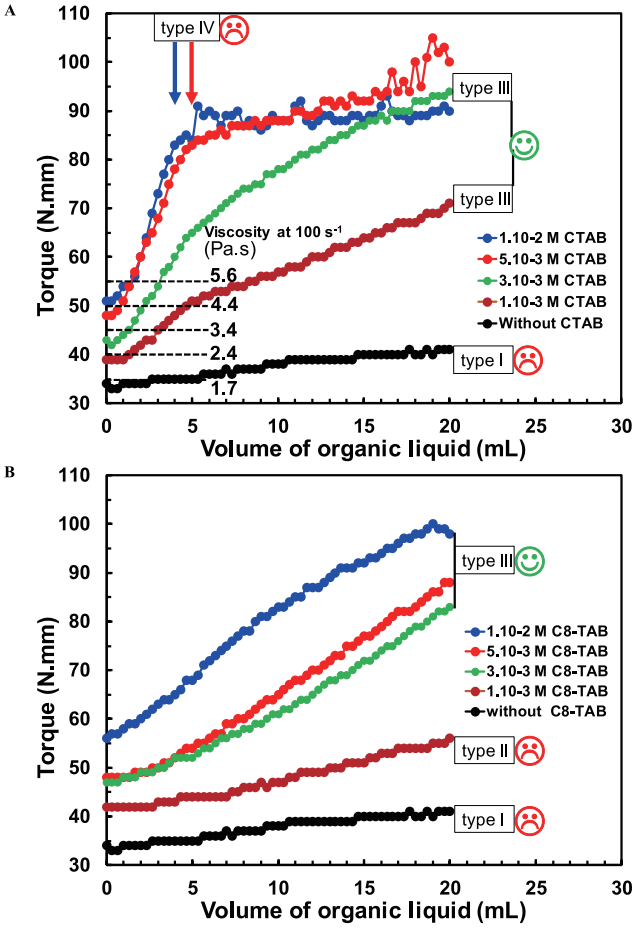

Fig. 5 Torque (N·mm) variation versus addition of TBP/Dodecane volume (mL) in fresh geopolymer suspension added at a flow rate of 4.0 mL.min^{-1} at a stirring speed of 800 rpm in fresh geopolymer in order to obtain 80 mL final hardened composite. Concentration of quaternary ammonium salts (CTAB or C16-TAB for A, and C8-TAB for B) in the activating solution are 0, 1, 3, 5 and 10.10^{-3} M.

of 20 mL of oil is completed, the torque reaches a certain value (60-90 N·mm, ≈ 10 Pa·s) and increases further, leading to successful incorporation. For the highest concentrations of CTAB (5.10^{-3} M and 10.10^{-3} M), the torque increases too quickly up to 85 N·mm at only 5 mL of incorporated OL. At this stage, the viscosity is so high (around 20 Pa·s) that the stirring of the impeller can no longer drive the geopolymer from the outside towards the center of the reactor. Thus, the organic liquid can no longer penetrate inside the geopolymer and accumulates on the surface of the slurry. In such a case, the torque signal is very noisy and the mixture heterogeneous (type IV GEOIL).

For C_8-TAB concentrations of 1.10^{-3} M, a positive effect is observed since the torque increases. However, this increase (from 30 to 40 N·mm) is not sufficient for allowing

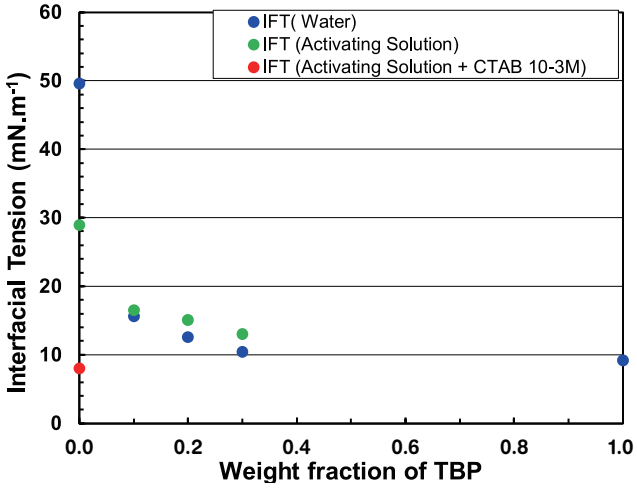

Fig. 6 Interfacial tension (mN·m^{-1}) at 25℃ between water (●) and activating solution (●) as a function of TBP content in TBP/Dodecane mixture.

correct oil incorporation (type II GEOIL). For the last three concentrations tested (3.10^{-3}, 5.10^{-3} M and 10.10^{-3} M), the torque varies in parallel with the same slope leading to good incorporation (type III GEOIL). On the other hand, in the presence of TBP/Dodecane, the CTAB seems to be more effective because the GEOILs viscosity increases much more than with the C_8-TAB. In fact, only type II or III GEOILs could be obtained with the C_8-TAB, and not type IV as observed with the CTAB.

Four other quaternary ammoniums salts (QAs) with different chain lengths (C_6, C_{10}, C_{12}, C_{14}) were also studied (data not shown) with the same concentrations and similar results were obtained.

3.3 Interfacial tension between (TBP/Dodecane) and aqueous phases

Figure 3 shows that increasing the percentage of TBP in the TBP/dodecane mixture enhances the quality of incorporation of the organic liquid into the geopolymer. In fact, the incorporation is of type I with 70% dodecane and 30% TBP, and of type II with TBP alone. To explain this phenomenon, interfacial tensions (Fig. 6) between different TBP/dodecane mixtures and aqueous solutions (water or the alkaline activating solution) are measured.

Figure 6 (blue points) illustrates that the measured interfacial tension, γ (mN·m^{-1}), between dodecane and water is 48 mN·m^{-1}, which is close to previously reported values of about 52 mN·m^{-1} (Table 1). Such a difference has already been observed and can be due to the different levels of purity of the dodecane, used either directly or after purification on alumina or silica columns[45]. γ then drops sharply to 17 mN·m^{-1} for 30% TBP and decreases steadily to 8 mN·m^{-1} for 100% TBP. This last value is consistent with the literature (12 mN·m^{-1} for 35% TBP[28] and 8[46] and 6.8 mN·m^{-1} [47]), for 100% TBP as mentioned in Table 2. It

Table 1 Interfacial tension between linear alkane (Cn) and water (20 or 25℃) reported in the literature. Values for Dodecane (C12) are represented in bold.

Alkane	Interfacial tension				
C5	49.0	50.3		50.9	
Cyclo-C6	50.0				45.0
C6	51.1	50.7	50.6	51.4	
C7	50.2	51.2	51.0	51.9	48.3
C8	50.8	51.5	51.4	52.5	
C9			51.8	52.4	
C10		52.0	52.1	53.2	
C11			52.4	53.1	
C12	**52.8**	**52.8**	**52.6**	**53.7**	
C13				54.0	
C14	52.2			54.5	
C16	53.3	53.3		55.2	
C10, 12, 14 kerosene					52.3
Reference	[50]	[51]	[52]	[45]	[49]

Table 2 Interfacial tension between mixture TBP (x)/alkane (1-x) and water (20 or 25℃) reported in the literature (x is the weight fraction of TBP in TBP/alkane).

Alkane	x	Interfacial tension ($mN \cdot m^{-1}$)	Reference
none	1.0	8	[46]
none	1.0	6.8	[47]
C7	0.0	48.3	[49]
	0.2	29.9	
	0.4	24.6	
	0.6	19.7	
	0.8	18.0	
	1.0	28.5	
C8	0.0	47.5	[53]
	0.21	21	
C12	0.0	52.6	[54]
	0.3	44.1	
C12	0.04	21	[28]
	0.35	12	

should be noted that some fluctuations are observed in the literature concerning the value of the surface tension between TBP/dodecane and water. This rapid decrease of γ with the increase of TBP percent in dodecane has already been observed for other TBP/alkane systems[28]. This confirms that TBP exhibits a surfactant effect, i.e., a few percent of TBP decreases the interfacial tension of the pure solvent.

Replacing the water by the activation solution (Fig. 6 (green points)) which is a very basic solution (pH = 14) of sodium silicate and sodium hydroxide, causes an initial significant drop in γ (from 48 to 29 $mN \cdot m^{-1}$) as already observed for the interfacial tension between dodecane and mixture of concentrated sodium hydroxide and silicate[48]. This indicates that even in the absence of QAs, silicates and HO^- anions reduce the interfacial tension. The addition of TBP further decreases γ down to a minimum of 9 $mN \cdot m^{-1}$ and gives a curve with a similar evolution as observed with water. The same value of γ is obtained for TBP weight fraction of 0.1, 0.2 and 0.3. It was not possible to measure γ for the TBP alone, because the refractive index of the TBP and the activation solution were too close, which did not allow to obtain a mathematical modelling of the shape of the interface. However, this tension can be estimated at around 8 $mN \cdot m^{-1}$ given that the drop formed tend to quickly come off the needle, as it is the case with water.

As expected (Fig. 6 red point), the addition in the activation solution of a QAs surfactant such as CTAB considerably decreases the interfacial tension to 8 $mN \cdot m^{-1}$ for 100% dodecane. As soon as TBP is added (for TBP > 0.1), the interfacial tension decreases further and is no longer measurable, because the drop comes off the needle immediately after being formed.

Values from the literature of interfacial tensions between linear alkane (C_n) and water at room temperature are repre-

sented in Table 1. It can be noted that γ increases slightly with the chain length of the alkane, since this value is around 49 $mN \cdot m^{-1}$ for pentane (C_5) and 55 $mN \cdot m^{-1}$ for hexadecane (C_{16}). Thus, a mixture of alkanes in C_{10}, C_{12}, C_{14} (kerosene) presents a γ of 52.3 $mN \cdot m^{-1}$ included between these 2 extreme values. Based on these interfacial tension values between water and the different alkanes, which are relatively close, it can be assumed that the interfacial tensions implying TBP-alkane mixtures should be close as well and do not depend on the type of alkane.

Table 2 presents interfacial tensions between mixtures of TBP (x)/alkane (1-x) and water found in the literature (x is the weight fraction of TBP in TBP/alkane). For x = 0, data are in agreement with those in Table 1. Also, γ decreases with increasing x value to a final value of 8 $mN \cdot m^{-1}$ [46] and 6.8 $mN \cdot m^{-1}$ [47] for x = 1, which is also in agreement with the value obtained in this work (9 $mN \cdot m^{-1}$). However slightly different value (28.5 $mN \cdot m^{-1}$) [49] for x = 1, has been also reported. For x = 0.1, 0.2 and 0.3, the values fluctuate a little more, which could be due to the significant water solubility in TBP (5.11×10^{-1} mol fraction) [47]. This could modify γ depending on the contact time between the drop of water at the end of the needle and the solution of TBP/Dodecane.

This hypothesis is confirmed by the fact that even though the solubility of TBP in water is quite low (2.70×10^{-5} mol fraction) [47] the action of TBP at the water/air interface is important since the surface tension of water saturated with TBP ($\gamma = 31.7$ $mN \cdot m^{-1}$) [49] is much lower than that of pure water ($\gamma = 72$ $mN \cdot m^{-1}$). In any case, the values obtained in this work are close to those reported in the literature [28].

In fact, TBP lowers the interfacial tension at the hydrocarbon/water interface whether the aqueous phase is pure or contains hydroxide and silicate ions. The minimum γ value is obtained for TBP weight fraction greater than x = 0.3.

TBP adsorbs at the alkane/water interface due to the basicity (nucleophilicity) of the oxygen atom due to the P = O functional group. The adsorption will then be governed by the ability of P = O groups to coordinate with water molecules. In the presence of acid in water (Ex: HNO_3), interactions are formed between the H^+ protons and the P = O group, making the P = O functions less available, hence increasing γ [28]. On the other hand, in a basic or neutral medium, the functional groups P = O remain available and γ decreases.

Figure 3 shows that TBP (Type II) incorporates better into the geopolymer than dodecane (Type I). Regarding the interfacial tension measurements (Fig. 6), this could be explained by lower γ values for TBP (around 8 $mN \cdot m^{-1}$) than for dodecane (29 $mN \cdot m^{-1}$), which facilitates the dispersion of TBP in the metakaolin suspension. The γ value for the TBP/Dodecane (30/70) mixture is equal to 14 $mN \cdot m^{-1}$ and is greater than that of TBP. This difference may be sufficient to explain that the incorporation of TBP/Dodecane is of type I, in contrast with the incorporation of TBP (type II).

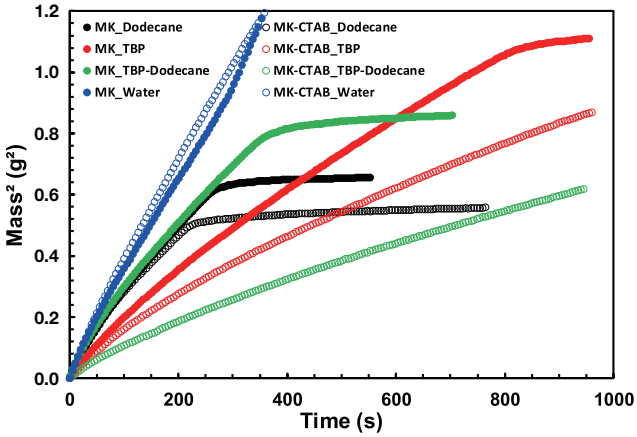

Fig. 7 Square of liquid mass (m^2) rising via capillarity versus time on metakaolin powders (natural MK) and impregnated with 10^{-2} M of CTAB (MK-CTAB). Liquids are water (blue circles), dodecane (black circles), TBP (red circles) and TBP/Dodecane (green circles). Full circles correspond to MK and open circles to MK-CTAB.

3.4 Washburn capillary rise method

To obtain information on the wettability of metakaolin by the different liquids investigated in this study, Washburn tests are performed. The rise of water, dodecane and TBP/Dodecane along conventional (MK) and hydrophobically modified (MK-CTAB) metakaolin are compared.

First, the metakaolin powder is packed into a cylindrical cell. Then, when the filter paper at the bottom of the cell is placed in contact with a liquid, the latter penetrates and rises along the powder by capillarity. The square weight of the cylinder cell is followed over time (Fig. 7), allowing the square of the liquid mass (m^2) rising via capillarity into the solid metakaolin to be described using the Washburn equation (Eq. 1).

$$m^2 = [C.\cos(\theta).\gamma.\rho^2/\eta].t \quad (1)$$

where m, C, θ, γ, ρ, η, t are the mass of liquid adsorbed, the capillary constant of the powder, the contact angle between the liquid and the solid, the superficial tension, the density, the viscosity of the liquid, and the time, respectively.

The curves (Fig. 7) are always made up of a first linear increasing evolution, which corresponds to the capillary rise of the liquid, followed by a plateau where m^2 no longer evolves, i.e., when the migration of liquid is over. As example, the plateau can be represented for dodecane (for 250 s) in Fig. 7 since it is quickly reached (for 250 s) and since the m^2 value (0.5 and 0.6 g^2) are not too large. On the

Table 3 Density ($kg.m^{-3}$), Viscosity (Pa·s), Superficial tension ($N.m^{-1}$) and $\rho^2.\gamma/\eta$ ($kg^2.m^{-3}.s^{-1}$) at 25℃ for water, dodecane and Finavestan oil. Slope ($\Delta m^2/\Delta t$ in $kg^2.s^{-1}$) and C.cos(θ) are extracted from the Washburn equation.

	Density at 25℃ (ρ)	Superficial Tension at 25℃ (γ)	Viscosity at 25℃ (η)	$\rho^2.\gamma/\eta$	Slope ($\Delta m^2/\Delta t$)	C.cos(θ)
	($kg.m^{-3}$)	($N.m^{-1}$)	($Pa\cdot s = N.s.m^{-2}$)	($kg^2.m^{-5}.s^{-1}$)	($kg^2.s^{-1}$)	(m^5)
Dodecane	749	0.0254	0.0018	7.92E+06	2.66E-09[a]	3.4E-16[a]
					2.55E-09[b]	3.2E-16[b]
TBP	977	0.0277	0.0036	7.34E+06	1.43E-09[a]	1.9E-16[a]
					1.00E-09[b]	1.4E-16[b]
TBP/dodecane	832	0.0248	0.0022	7.80E+06	2.72E-09[a]	3.5E-16[a]
					7.13E-10[b]	9.1E-17[b]
Water	1000	0.0725	0.001	7.25E+07	3.17E-09[a]	4.4E-17[a]
					3.21E-09[b]	4.4E-17[b]

[a] with metakaolin (MK), [b] with hydrophobic metakaolin (MK-CTAB)

other hand, for reasons of graphic representation the plateau is not represented in the opposite case (values of m^2 at the plateau too high or time to obtain the plateau too long).

Theoretically, the maximum volume of liquid filling the pores of the cylinder of metakaolin is constant. Hence, the higher the density of the liquid, the higher the values of m^2 at the plateau (Table 3). The most interesting part of these curves is the ascending part because the value of the slope characterizes the capillary rise during the steady state.

From the value of the slope and the knowledge of the density, viscosity and superficial tension[55] of each liquid, C.cos(θ)[56, 57] can be extracted using Eq. 1 (Table 3).

For water, the speed of migration is almost identical on the two kinds of metakaolin particles, which indicates that the interaction with the solid is not QAs dependent. This confirms that the hydrophobic alkyl-chain of quaternary ammoniums fixed at the surface of metakaolin particles has no interaction with water. In the absence of CTAB, the slope of the function $m^2 = f(t)$ is the least important for TBP, but this difference does not seem sufficient to explain the different behavior of the TBP during incorporation into the geopolymer (Type II) in comparison with the incorporation of dodecane and TBP/Dodecane (Type I).

In the case of the CTAB-modified metakaolin, the rate of TBP migration significantly decreases. This could explain the different behavior observed between the incorporation of TBP and dodecane in the geopolymer. As for TBP, the capillary rise of TBP/dodecane decreases on the treated metakaolin powder, which does not explain their different incorporation behavior (Type I for TBP/Dodecane and Type II for TBP).

Overall, Washburn rising tests show that all tested liquids are capable of wetting metakaolin particles, since capillary rises are observed. These capillary interactions presented on Fig. 7 highlight the importance of the interactions between metakaolin particles and liquid phases. When metakaolin particles areimpregnated with CTAB, their interactions with liquids containing TBP decreases, while remaining unchanged with water.

4 Conclusion

Torque monitoring during organic liquids (OL) incorporation into geopolymer (GP) suspensions provides information on the viscosity of the reaction mixture using a prior torque/viscosity calibration curve. This avoids off-line rheological measurements when varying the process (stirring, time, ...) and/or the formulation (nature and quantity of QAs, ..) parameters. Four types of torque evolution, corresponding to four types of GEOIL consistencies have been observed (Type I, II, III and IV). A continuous increase in torque corresponds to an efficient incorporation of OL into the geopolymer (Type III). If the torque remains constant, the OL is not incorporated and remains at the surface of the geopolymer slurry (Type I). According to Type I and III, if the torque remains constant after an initial increase, Type II GEOIL is obtained with the excess of OL remaining at the surface. Finally, an excessive increase in torque during the incorporation process no longer allows the stirring of the medium (Type IV).

When facing type I, quaternary alkylammonium salts such as CTAB can be used to obtain a regular torque increase, leading to an efficient OL incorporation. Shorter alkyl chains QAs such as hexyl or octyl trimethylammonium bromide can also be employed, although with less efficiency than CTAB, since higher concentrations are required to obtain similar performances.

Without surfactants, the incorporation of TBP (Type II)

into fresh geopolymers is easier than the incorporation of dodecane (Type I). Regarding interfacial tension measurements between OLs and the aqueous alkaline activating solutions, lower values are obtained for TBP ($8\ mN \cdot m^{-1}$) than for dodecane ($29\ mN \cdot m^{-1}$). This explains the easier dispersion of TBP in metakaolin suspensions. In addition, the gamma value for the TBP30/Dodecane70 mixture ($14\ mN \cdot m^{-1}$) is higher than the one of TBP, which may explain that the incorporation of TBP/Dodecane is of Type I, while the one of TBP is of Type II.

Finally, the Washburn capillary method highlighted that the hydrophobic alkyl-chain of quaternary ammoniums fixed at the surface of metakaolin particles has no interaction with water. On the over hand, the rate of TBP migration slows down if metakaolin particles are previously treated with CTAB (compared with untreated particles) and this unlike dodecane. This could be part of the answer to explain the difference in behavior between the incorporation of TBP and dodecane in the geopolymer.

Acknowledgments

Chevreul Institute (FR 2638), Ministère de l'Enseignement Supérieur et de la Recherche, Région Hauts de France, and FEDER are acknowledged for supporting and funding part of this work.

References

1) Davidovits, J. Geopolymers: Inorganic polymeric new materials. *J. Therm. Anal.* **37**, 1633-1656 (1991).
2) Duxson, P.; Fernández-Jiménez, A.; Provis, J.L.; Lukey, G.C.; Palomo, A.; van Deventer, J.S.J. Geopolymer technology: The current state of the art. *J. Mater. Sci.* **42**, 2917-2933 (2007).
3) Provis, J.L.; van Deventer, J.S.J. eds. *Geopolymers: Structure, Processing, Properties and Industrial Applications*, Woodhead Publishing Ltd. (2009).
4) Andrew, R.M. Global CO_2 emissions from cement production, 1928-2018. *Earth Syst. Sci. Data* **11**, 1675-1710 (2019).
5) Nestle, N.; Zimmermann, C.; Dakkouri, M.; Niessner, R. Action and distribution of organic solvent contaminations in hydrating cement: Time-resolved insights into solidification of organic waste. *Environ. Sci. Technol.* **35**, 4953-4956 (2001).
6) Pollard, S.J.T.; Montgomery, D.M.; Sollars, C.J.; Perry, R. Organic compounds in the cement-based stabilisation/solidification of hazardous mixed wastes—Mechanistic and process considerations. *J. Hazard. Mater.* **28**, 313-327 (1991).
7) Bai, C.; Colombo, P. Processing, properties and applications of highly porous geopolymers: A review. *Ceram. Int.* **44**, 16103-16118 (2018).
8) Hasnaoui, A.; Reeb, C.; De Campos, M.; Davy, C.; Lambertin, D. Controlling the properties of metakaolin-based geopolymer/liquid organic waste emulsions: A rheological approach. *Appl. Clay Sci.* **245**, 107160-107169 (2023).
9) Bai, C.; Franchin, G.; Elsayed, H.; Conte, A.; Colombo, P. High strength metakaolin-based geopolymer foams with variable macroporous structure. *J. Eur. Ceram. Soc.* **36**, 4243-4249 (2016).
10) Barbosa, T.R.; Foletto, E.L.; Dotto, G.L.; Jahn, S.L. Preparation of mesoporous geopolymer using metakaolin and rice husk ash as synthesis precursors and its use as potential adsorbent to remove organic dye from aqueous solutions. *Ceram. Int.* **44**, 416-423 (2018).
11) Cilla, M.S.; de Mello Innocentini, M.D.; Morelli, M.R.; Colombo, P. Geopolymer foams obtained by the saponification/peroxide/gelcasting combined route using different soap foam precursors. *J. Am. Ceram. Soc.* **100**, 3440-3450 (2017).
12) Glad, B.E.; Kriven, W.M. Highly porous geopolymers through templating and surface interactions. *J. Am. Ceram. Soc.* **98**, 2052-2059 (2015).
13) Medpelli, D.; Seo, J.-M.; Seo, D.-K. Geopolymer with hierarchically meso-/macroporous structures from reactive emulsion templating. *J. Am. Ceram. Soc.* **97**, 70-73 (2014).
14) Cantarel, V.; Lambertin, D.; Poulesquen, A.; Leroux, F.; Renaudin, G.; Frizon, F. Geopolymer assembly by emulsion templating: Emulsion stability and hardening mechanisms. *Ceram. Int.* **44**, 10558-10568 (2018).
15) Cantarel, V.; Nouaille, F.; Rooses, A.; Lambertin, D.; Poulesquen, A.; Frizon, F. Solidification/stabilisation of liquid oil waste in metakaolin-based geopolymer. *J. Nucl. Mater.* **464**, 16-19 (2015).
16) Lambertin, D.; Cantarel, V.; Poulesquen, A.; Frizon, F. Production of geopolymer composites comprising organic phase change materials. 36pp.; Chemical Indexing Equivalent to 168:476290 (FR) (2018).
17) Liu, J.; Li, F.; Zhang, R.; Dong, E.; Gong, X. *et al.* Foam geopolymer for tunnel composite lining and preparation method thereof. 6pp. (2018).
18) Cantarel, V. Etude de la synthèse de composites liquides organiques/géopolymère en vue du conditionnement de déchets nucléaires (2016).
19) Akay, G.; Tong, L. Preparation of colloidal low-density polyethylene latexes by flow-induced phase inversion emulsification of polymer melt in water. *J. Colloid Interface Sci.* **239**, 342-357 (2001).
20) Akay, G. Flow-induced phase inversion in the intensive processing of concentrated emulsions. *Chem. Eng. Sci.* **53**, 203-223 (1997).
21) Saw, L.K.; Brooks, B.W.; Carpenter, K.J.; Keight, D.V.

Catastrophic phase inversion in region II of an ionomeric polymer-water system. *J. Colloid Interface Sci.* **279**, 235-243 (2004).
22) Catte, M.; Ontiveros, J.F.; Aramaki, K.; Pierlot, C. Catastrophic emulsion inversion process of highly viscous isosorbide biobased polyester monitored in situ by torque and light backscattering. *J. Oleo Sci.* **67**, 925-931 (2018).
23) Pierlot, C.; Ontiveros, J.F.; Royer, M.; Catte, M.; Salager, J.-L. Emulsification of viscous alkyd resin by catastrophic phase inversion with nonionic surfactant. *Colloids Surf. A* **536**, 113-124 (2018).
24) Song, D.; Zhang, W.; Gupta, R.K.; Melby, E.G. Role of operating conditions in determining droplet size and viscosity of tackifier emulsions formed via phase inversion. *AIChE J.* **57**, 96-106 (2011).
25) Goger, A.; Thompson, M.R.; Pawlak, J.L.; Lawton, D.J.W. *In situ* rheological measurement of an aqueous polyester dispersion during emulsification. *Ind. Eng. Chem. Res.* **54**, 5820-5829 (2015).
26) Galindo-Alvarez, J.; Sadtler, V.; Choplin, L.; Salager, J.-L. Viscous oil emulsification by catastrophic phase inversion: Influence of oil viscosity and process conditions. *Ind. Eng. Chem. Res.* **50**, 5575-5583 (2011).
27) Edward, A.C.; Sadtler, V.; Marchal, P.; Choplin, L.; Delfosse, F.; Maze, M. Preparation of highly concentrated bitumen emulsions by catastrophic phase inversion: Follow-up of the emulsification process. *Colloids Surf. A* **458**, 25-31 (2014).
28) Nave, S.; Mandin, C.; Martinet, L.; Berthon, L.; Testard, F. *et al.* Supramolecular organisation of tri-*n*-butyl phosphate in organic diluent on approaching third phase transition. *Phys. Chem. Chem. Phys.* **6**, 799 (2004).
29) Reeb, C.; Pierlot, C.; Davy, C.; Lambertin, D. Incorporation of organic liquids into geopolymer materials - A review of processing, properties and applications. *Ceram. Int.* **47**, 7369-7385 (2021).
30) Pierlot, C.; Hu, H.; Reeb, C.; Bassetti, J.; Bertin, M. *et al.* Selection of suitable surfactants for the incorporation of organic liquids into fresh geopolymer pastes. *Chem. Eng. Sci.* **255**, 117635 (2022).
31) Petlitckaia, S.; Poulesquen, A. Design of lightweight metakaolin based geopolymer foamed with hydrogen peroxide. *Ceram. Int.* **45**, 1322-1330 (2019).
32) Dong, T.; Xie, S.; Wang, J.; Zhao, G.; Song, Q. Solidification and Stabilization of Spent TBP/OK Organic Liquids in a Phosphate Acid-Based Geopolymer. *Sci. Technol. Nucl. Install.* **2020**, 1-7 (2020).
33) Reeb, C.; Davy, C.A.; Pierlot, C.; Bertin, M.; Cantarel, V.; Lambertin, D. Emulsification of low viscosity oil in alkali-activated materials. *Cem. Concr. Res.* **162**, 106963 (2022).
34) Campos, M.D.; Reeb, C.; Davy, C.A.; Hosdez, J.; Lambertin, D. Solidification/stabilization (S/S) of high viscosity organics in geopolymers. *J. Nucl. Mater.* **571**, 153979 (2022).
35) Kang, F.; Wang, Q.; Xiang, S. Synthesis of mesoporous Al-MCM-41 materials using metakaolin as aluminum source. *Mater. Lett.* **59**, 1426-1429 (2005).
36) Pei, Y.-R.; Yang, J.-H.; Choi, G.; Choy, J.-H. A geopolymer route to micro- and meso-porous carbon. *RSC Adv.* **10**, 6814-6821 (2020).
37) Singhal, A.; Gangwar, B.P.; Gayathry, J.M. CTAB modified large surface area nanoporous geopolymer with high adsorption capacity for copper ion removal. *Appl. Clay Sci.* **150**, 106-114 (2017).
38) Yu, Z.; Song, W.; Li, J.; Li, Q. Improved simultaneous adsorption of Cu (II) and Cr (VI) of organic modified metakaolin-based geopolymer. *Arab. J. Chem.* **13**, 4811-4823 (2020).
39) Chen, S.; Qi, Y.; Cossa, J.J.; Salomao, D.S.I.D. Efficient removal of radioactive iodide anions from simulated wastewater by HDTMA-geopolymer. *Prog. Nucl. Energy* **117**, 103112 (2019).
40) Falah, M.; MacKenzie, K.J.; Knibbe, R.; Page, S.J.; Hanna, J.V. New composites of nanoparticle Cu (I) oxide and titania in a novel inorganic polymer (geopolymer) matrix for destruction of dyes and hazardous organic pollutants. *J. Hazard. Mater.* **318**, 772-782 (2016).
41) Montgomery, D.M.; Sollars, C.J.; Perry, R. Optimization of cement-based stabilization/solidification of organic-containing industrial wastes using organophilic clays. *Waste Manag. Res.* **9**, 21-34 (1991).
42) Siyal, A.A.; Shamsuddin, M.R.; Khan, M.I.; Rabat, N.E.; Zulfiqar, M. *et al.* A review on geopolymers as emerging materials for the adsorption of heavy metals and dyes. *J. Environ. Manage.* **224**, 327-339 (2018).
43) Cantarel, V. Etude de la synthèse de composites liquides organiques/géopolymère en vue du conditionnement de déchets nucléaires. (Université Blaise Pascal-Clermont-Ferrand II, 2016).
44) Revathi, T.; Jeyalakshmi, R.; Rajamane, N.P.; Sivasakthi, M. Evaluation of the role of Cetyltrimethylammoniumbromide (CTAB) and Acetylenicglycol (AG) admixture on fly ash based geopolymer. *Orient. J. Chem.* **33**, 783-792 (2017).
45) Goebel, A.; Lunkenheimer, K. Interfacial tension of the water/*n*-alkane interface. *Langmuir* **13**, 369-372 (1997).
46) Sagert, N.H.; Sagert, N.H.; Quinn, M.J.; Lee, W. Adhesion at the tributylphosphate—water interface. *J. Colloid Interface Sci.* **74**, 564-566 (1980).
47) Yoon, H.; Oostrom, M.; Werth, C.J. Estimation of interfacial tension between organic liquid mixtures and water. *Environ. Sci. Technol.* **43**, 7754-7761 (2009).
48) Bertin, M.; Rodrigues, D.G.; Pierlot, C.; Albert-Mercier,

C.; Davy, C. *et al.* Influence of cetyltrimethylammonium bromide and hydroxide ions on the interfacial tension and stability of emulsions of dodecane in aqueous silicate solutions. *Colloids Surf. A Physicochem. Eng. Asp.* **628**, 127306(2021).
49) Wongsawa, T.; Koonsang, T.; Kunthakudee, N.; Prapasawat, T.; Maneeintr, K.; Pancharoen, U. The experimental investigations on viscosity, surface tension, interfacial tension and solubility of the binary and ternary systems for tributyl phosphate(TBP)extractant in various organic solvents with water: Thermodynamic NRTL model and molecular interaction approach. *J. Mol. Liq.* **251**, 229-237(2018).
50) Demond, A.H.; Lindner, A.S. Estimation of interfacial tension between organic liquids and water. *Environ. Sci. Technol.* **27**, 2318-2331(1993).
51) Johnson, R.E.; Dettre, R.H. The wettability of low-energy liquid surfaces. *J. Colloid Interface Sci.* **21**, 610-622(1966).
52) Zeppieri, S.; Rodríguez, J.; López De Ramos, A.L. Interfacial tension of alkane + water systems. *J. Chem. Eng. Data* **46**, 1086-1088(2001).
53) Prochaska, K.; Staszak, K. Adsorption at the liquid/liquid interface in mixed systems with hydrophobic extractants and modifiers 1. Study of equilibrium interfacial tension at the hydrocarbon/water interface in binary mixed systems. *J. Colloid Interface Sci.* **285**, 1-8(2005).
54) Bajoria, S.L.; Rathod, V.K.; Pandey, N.K.; Mudali, U.K.; Natarajan, R. Effect of tri-*n*-butyl phosphate on physical properties of dodecane–nitric acid system. *J. Radioanal Nucl. Chem.* **295**, 271-276(2013).
55) Vo, Q.N.; Dang, L.X.; Nguyen, H.D.; Nilsson, M. Microscopic behaviors of tri-*n*-butyl phosphate, *n*-dodecane, and their mixtures at air/liquid and liquid/liquid interfaces: An AMBER polarizable force field study. *J. Phys. Chem. B* **123**, 655-665(2019).
56) Galet, L.; Patry, S.; Dodds, J. Determination of the wettability of powders by the Washburn capillary rise method with bed preparation by a centrifugal packing technique. *J. Colloid Interface Sci.* **346**, 470-475(2010).
57) Kirdponpattara, S.; Phisalaphong, M.; Newby, B.Z. Applicability of Washburn capillary rise for determining contact angles of powders/porous materials. *J. Colloid Interface Sci.* **397**, 169-176(2013).